

# Decentralized Energy Storage with Metal Hydride – Phase Change Material Hybrid Systems<sup>#</sup>

Marco Maggini<sup>1</sup>, Simone Pennesi<sup>1</sup>, Piergiovanni Domenighini<sup>2</sup>, Andrea Luigi Facci<sup>1\*</sup>, Stefano Ubertini<sup>1</sup>

<sup>1</sup> Department of Economics, Engineering, Society and Business Administration, University of Tuscia, 01100 Viterbo, Italy

<sup>2</sup> Ricerca sul Sistema Energetico RSE S.p.a., 00197 Roma, Italy

(Corresponding Author: [andrea.facci@unitus.it](mailto:andrea.facci@unitus.it))

## ABSTRACT

Seasonal energy storage may represent an important step for the energy transition, reducing both energy consumption and greenhouse gas emissions. This paper presents an analysis of an integrated energy system designed to power a building by combining energy production and storage. The system studied in this paper consists of photovoltaic panels, an electrolyzer to convert excess energy into hydrogen, a metal hydride tank, and a fuel cell for reconversion to electricity. The aim of this paper is to evaluate the energetic and economic performance of this system under various climatic scenarios and for different storage capacities. The results demonstrate that the system can overcome the seasonal mismatch between production and consumption of a 1-apartment building, with a self-sufficiency ratio > 98% and a PV system < 6kW. Economic-wise, the system needs an initial investment of ~120 k€ and a payback period 11 ÷ 22 years depending on the storage capacity, thus confirming substantial challenges for the scalability of metal hydrides in residential buildings. Their cost accounts for nearly 38% of the total investment costs.

**Keywords:** renewable energy resources, hydrogen technologies, mitigation technologies, metal hydrides, energy systems, climate change

## 1. INTRODUCTION

The necessity to mitigate climate changes and the increasing demand of clean energy have accelerated the global transition towards renewable energy sources (RES). RES like solar and wind power offer a sustainable alternative to fossil fuels, but their intermittency poses a significant challenge to grid stability and energy reliability. To overcome this limitation, energy storage solutions are crucial for decoupling energy production from consumption. The integration of solar photovoltaic

systems in buildings has evolved significantly over recent decades, driven by technological advancements, policy incentives, and growing environmental awareness. In Fig.1 [1] the evolution of rooftop and utility-scale PV power plants in the EU is shown. From 2016 to 2022, we witnessed a nearly 9-fold global increase. Small applications require small investment compared to large scale power plant and are quicker to build, thus explaining the bigger evolution year after year.

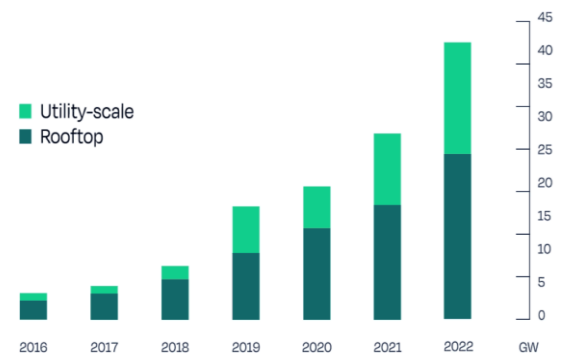


Fig. 1. Annual PV rooftop and utility scale in EU [1].

Battery Energy Storage Systems (BESS) are emerging as a vital component for enhancing the resilience and self-sufficiency of buildings. Integrating BESS allow building owners to store surplus solar energy generated during the day and use it during periods of high demand or when solar generation is low, such as at night. Early studies, such as Goebel et al. [2], highlighted a significant challenge, concluding that at the prevailing battery module prices, investments in residential BESS were not profitable if used solely as a buffer for solar energy. A more recent techno-economic analysis by Rosati et al. [3], showed that a correctly sized lithium-ion battery can indeed lead to a sustainable investment for residential buildings across various climates. Their work confirmed that, from a techno-economic standpoint, BESS are more

<sup>#</sup> This is a paper for the 17th International Conference on Applied Energy (ICAE2025), December 8-12, 2025, Bangkok, Thailand.

effective for daily energy storage than for seasonal storage, as the high costs make long-term storage investments unsustainable. Both studies suggest that a singular focus on self-consumption is not sufficient to fully utilize the potential of BESS. To overcome the problem of seasonal storage, Linkgkang et al. [4] analyzed a hybrid system with BESS and electrolyzer, reaching good results in terms of energy storage. The major issue is the cost of the system. In order for the initial investment to return, the price of hydrogen must be between 12 and 19 €/kg, while the European hydrogen observatory tool [5] estimates the cost of hydrogen with PV system at 6.9 €/kg in the same area studied in the paper. Evangelos et al. [6] studied a system with electrolyzer, hydrogen storage system and fuel cell. The authors analyzed the performance of a zero-energy building in Athens, Greece, and found that a photovoltaic system of 203 m<sup>2</sup> combined with a 34 m<sup>3</sup> hydrogen storage capacity can make a building of 400 m<sup>2</sup> with six occupants completely autonomous for one year. Abdolmaleki et al. [7] explored the techno-economic feasibility of a hybrid energy storage system combining hydrogen metal hydride (MHS) and battery energy storage (BESS) for a PV-powered commercial building in the Mediterranean climate. Using dynamic simulations and response surface methodology (RSM) for optimization, the research identifies optimal component sizing to achieve off-grid electrification and net-zero energy. Magnesium is used as MH, while an active cooling/heating system is employed to facilitate the kinetics of the reactions.

The present project aims to build upon the results of Rosati et al. [3] and expand the horizon of utility-scale storage systems to hydrogen, specifically solid-state solutions coupled with small-scale electrolyzers and fuel cells. We analyze the same climate zones focusing on the evaluation of the economic feasibility and we draw a comparison with traditional BESS. To the best of our knowledge, literature lacks a sensitivity analysis to climate zones for a zero-emission residential building employing solely MH-PCM hydrogen storage systems, i.e., passively managed and with higher efficiency. The rest of the paper is structured as follows: Sec. 2 presents the problem statement and the methodology employed to model the global production-storage system. Sec. 3 and Sec. 4 present and discuss the results, respectively, while Sec. 5 draws the conclusions and presents possible further developments of the work.

## 2. METHODOLOGY

### 2.1 System description

The system is depicted in Fig. 2 and comprises of: a rooftop PV module, a DC-DC converter unit, an electrolyzer, a hydrogen storage system, a fuel cell, a DC-AC inverter unit, and the heat pump which supplies heating and cooling energy according to the consumption of the building. Consumption curves are retrieved from [3] to ensure consistency between the two analyses. Whenever the energy generated from the PV module is larger than the system can collect, i.e., when the net generated power  $P_{net}$ :

$$P_{net} = PV_h \eta_{DC} - \frac{C_h}{\eta_{inv}} > 0,$$

the excess is stored in the MH system, if possible. Otherwise, it is sold to the grid.  $PV_h$  is the hourly photovoltaic production [W], while  $C_h$  is the hourly consumption [W]. Similarly, if the energy required by the system fuel cell – heat pump is larger than the energy provided by the PV and/or the hydrogen storage system, additional energy is retrieved from the grid.

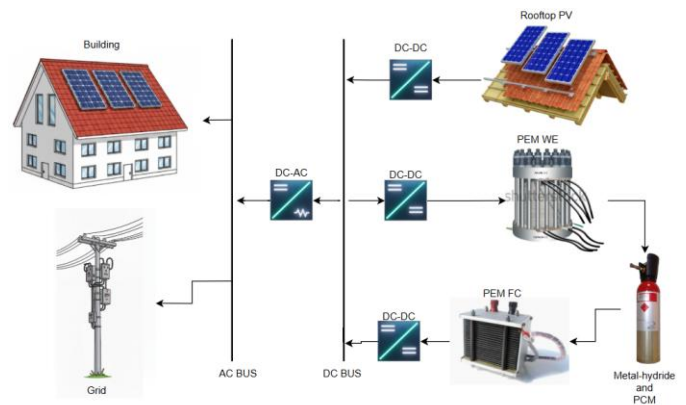


Fig. 2. Conceptualization of the analyzed system.

A baseline scenario of a 101 m<sup>2</sup> apartment located in central Italy (Rome), with a yearly consumption of 4,306 kWh is considered. The sensitivity analysis will change the number of apartments, the location (i.e., climate), and size of the storage system. Four other locations are considered to iterate on the climate zones, namely Warsaw, Athens, Malaga, and Larnaca, representative of the four climate zones, i.e., cold, cooling based, moderate, and hot. The baseline scenario in Rome analyzes a heating-based climate. We use the classification set in [8].

### 2.2 Photovoltaic system

We retrieve the hourly PV generation of the five climate zones from PVGIS. We set system losses to 14% (including DC-DC converter efficiency) and the DC-AC

inverter efficiency to 91%. We size the PV peak power so as to comply with the following equation:

$$\frac{1}{\phi} \int_0^T PV_h dt + \frac{\eta_{rt}}{1 - \phi} \int_0^T PV_h dt = \frac{1}{\eta_{inv}} \int_0^T C_h dt,$$

where  $\phi$  is the self-consumed fraction of the generated energy and  $\eta_{rt}$  is the average round-trip efficiency of the storage system, set to 50% and equal to the combination of the electrolyzer and fuel cell average efficiencies. Such efficiencies are described in later sections of the paper. We thus ensure that the energy generated by the PV is approximately equal to the required yearly energy.

### 2.3 Electrolyzer Module

We use a Polymer Electrolyte Membrane Electrolyzer with a nominal power of 4 kW. The electrolyzer curve used in this project is covered by copyright, so it won't be shown. This curve (like the Fuel Cell curve shown in fig.4) represents the correlation between the efficiency of the electrolyzer and the set point. The efficiency is the ratio between the chemical energy produced and the power consumption, while the set point is the ratio between the operating power and the nominal one. The characteristic curve of the electrolyzer is retrieved from experimental data. Another important parameter is the net Power of the cell,  $P = PV_{hourly} \cdot \eta_{DC} - E_{building}/\eta_{inv}$ , equal to the difference between the energy generated by the PV modules ( $PV_{hourly}$ ) and the building consumption rates ( $E_{building}$ ). The hydrogen is generated at the electrolyzer at the pressure of  $p_{H_2}^{EL} = 15$  bar and gets immediately compressed in a lab-scale piston compressor to  $p_{H_2}^a = 50$  bar before going into the buffer volume. We assume the buffer volume big enough to disregard any variation in pressure with time. In other words, any possible excess in hydrogen production ends up in the buffer volume without altering its storage pressure. The number of electrolyzers  $n_{EL}$  is calculated as follows:

$$n_{EL} = \text{ceil} \left[ \max \left( \frac{P_{net}}{4 \text{ kW}} \right) \right].$$

### 2.4 Hydrogen Storage Module

The individual  $H_2$  storage module is made of an inner cylinder of MH (Hydralloy C5 [9]), with porosity  $\xi = 0.5$ , length  $L = 1.27$  m, and diameter  $D = 2.54$  cm (see Fig. 3). Such a configuration has been retrieved by previous research of the authors [10-13] which describes it as the recommended layout to store 1.16 kWh of

energy. A gravimetric density  $w = \frac{m_{H_2}}{m_{MH}} = \frac{S_C \cdot M_{H_2}}{M_{MH}} = 1.81\%$  is used. The MH cylinder is surrounded by an external jacket of PCM (Paraffin RT30), with external radius  $b_2$ .

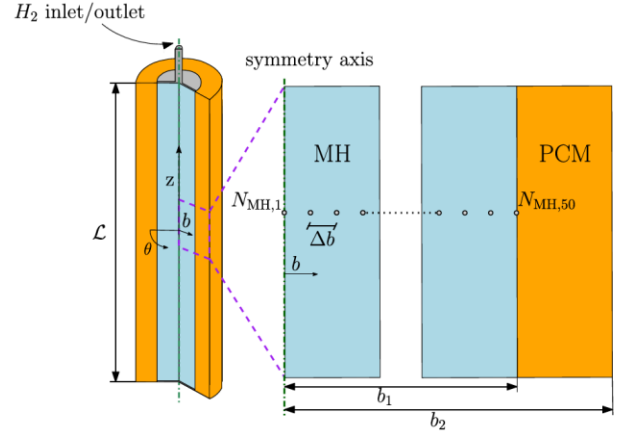


Fig. 3. MH-PCM hydrogen storage system scheme.

During the charge phase, hydrogen is supplied at the inlet pressure  $p_{H_2}^a = 50$  bar from the compressor. During discharge, the outlet hydrogen pressure is set to  $p_{H_2}^d = 1$  bar, equal to the FC operating pressure. The hydrogen storage system is composed of a series of autonomous MH-PCM modules, under the assumption that each works independently. Therefore, the outlet mass flow rate from the electrolyzer is evenly split between the  $n$  storage modules. Similarly, the output mass flow rate from the reservoir to the FC is evenly split between the  $n$  storage modules.

We make use of the following hypotheses to build out mathematical model: (i) gases are ideal and compressible; (ii) the porous medium is homogeneous; (iii) the thermos-physical properties of both MH and PCM are not a function of temperature; (iv) the pressure inside the vessel is homogeneous in space and constant in time ( $p = p_{H_2}$ ); (v) MH and the hydrogen gas are in local thermal equilibrium; (vi) the natural convection within the PCM is neglected. We base our mathematical conceptualization on the mass and energy conservation inside the MH domain, as follows [14]:

$$\frac{dm_{H_2}}{dt} = f_{H_2} - r \cdot m_{MH} \cdot w,$$

$$\frac{\partial T}{\partial t} = \alpha_{MH}^e \nabla^2 T + \dot{q}.$$

$m_{H_2}$  is the amount of gaseous hydrogen inside the individual storage module,  $f_{H_2}$  is the hydrogen mass flow rate (positive during the charge phase and negative in the discharge phase),  $r$  is the hydrogenation reaction

rate,  $m_{MH}$  is the hydride total mass,  $w$  is the hydride gravimetric density,  $T$  is the hydride local temperature,  $\alpha_{MH}^e$  is the hydride effective thermal diffusivity, and  $\dot{q}$  is the reaction heat source (positive during the charge phase and negative in the discharge phase). In turn, the reaction rate  $r$  is:

$$r = C e^{-\frac{E}{RT}} \cdot p_r \cdot \phi_r,$$

where  $C$  and  $E$  are kinetics constants (different for charge and discharge),  $p_r = \ln\left(\frac{p_{H_2}}{p_{eq}}\right)$  in charge and  $\frac{p_{H_2} - p_{eq}}{p_{eq}}$  in discharge, and  $\phi_r = 1 - \frac{m_{H_2}}{m_{MH}}$  in charge and  $\frac{m_{H_2}}{m_{MH}}$  in discharge. The equilibrium pressure  $p_{eq}$  is a function of the reaction enthalpy and entropy variations ( $\Delta H$  and  $\Delta S$ , respectively) and  $\phi = \frac{m_{H_2}}{m_{MH}}$  according to the Van't Hoff equations.

To ensure faster and deeper desorption, the MH-PCM vessel is surrounded by a 100 W electric heater. The system activates whenever the PCM surface temperature falls below the phase change temperature, i.e., 300 K. The energy for its activation is retrieved from the grid, thus slightly but negligibly reducing the round-trip efficiency.

## 2.5 Fuel Cell Module

We use a Polymer Electrolyte Membrane Fuel Cell with a nominal power of 27.1 kW. The characteristic experimental curve of the fuel cell is reported in Fig. 4 [15]. The number of Fuel Cells to be used in parallel to ensure maximum efficiency is as follows:

$$n_{FC} = \text{ceil} \left[ - \min \left( \frac{P_{net}}{27.1 \text{ kW}} \right) \right].$$

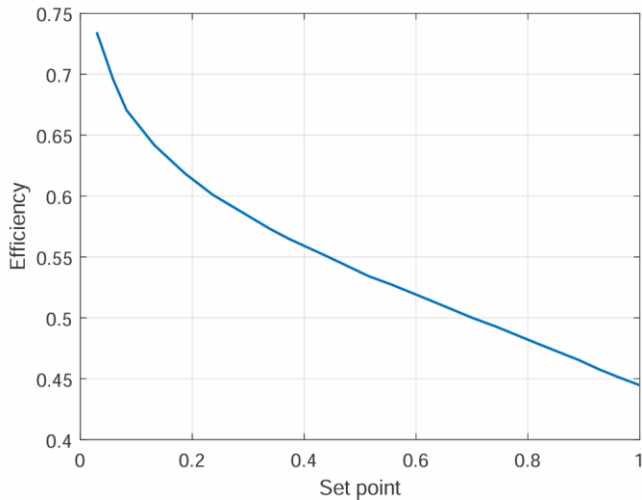


Fig. 4. Fuel Cell efficiency curve, adapted from [15]. Horizontal axis represents the ratio between actual power and nominal power. The

vertical axis represents the efficiency calculated as the ratio between output electric power and input chemical power (fuel).

## 2.6 Power converter units and heat pumps

The PV-PEMEL coupling requires a DC-DC converter unit. We assume an efficiency of 86%. A DC-AC inverter unit is located before the building's grid, after the PV module and the FC module, with an efficiency of 91%. We assume a coefficient of performance equal to 2.5 in heating mode and 1.5 in cooling mode for the heat pump.

## 2.7 Costs

A fixed cost of  $G_e = 0.25$  €/kWh is used for the grid electricity (either sold or purchased), since it is the average price in the EU as of 2024 S2 [16]. The payback period of the investments on the MH storage system PBP is calculated as follows:

$$\text{PBP} = \frac{G_{MH}}{I_{\text{year}}},$$

where  $G_{MH}$  is the initial capital investment of the storage system and  $I_{\text{year}} = (E_{\text{year}} - E_{\text{grid}}^{\text{out}} + E_{\text{grid}}^{\text{in}} \cdot G_e)$  is the annual saving due to reduction in costs of electricity withdrawn from the grid.  $E_{\text{grid}}^{\text{out}}$  and  $E_{\text{grid}}^{\text{in}}$  are the energy retrieved from and sent to the grid, respectively.

Therefore, we define the Self Sufficiency Ratio (SSR) as follows:

$$\text{SSR} = 1 - \frac{E_{\text{grid}}^{\text{out}}}{E_{\text{year}}},$$

The SSR gives an estimate of the effectiveness of the hydrogen storage system and is equal to 1 when the yearly consumption of the residential building is covered by the storage system without retrieving energy from the grid.

## 2.8 Numerical Solution

The MH is discretized with 25 radial nodes, with a corresponding node-to-node distance of approximately 0.5 mm. The PCM is discretized maintaining the same node-to-node resolution of 0.5 mm. According to the complete axi-symmetry of the MH-PCM design, we only discretize the MH and the PCM domain along the radial direction. We use a second order finite difference scheme for the spatial discretization while the numerical solution of the differential and algebraic equations is implemented in Matlab R2024b.

The solution spans over 1 year (8760 points, each equal to 1 hour) and is looped over the main system parameters, e.g., the hydrogen storage size, the climate zones, and number of apartments. Iterating on the

climate zones change the PV nominal power and the building consumptions.

### 3. RESULTS AND DISCUSSION

#### 3.1 Baseline scenario

In the baseline scenario, we use a storage system of 500 modules and  $\phi = 0$ , thus all energy generated flows through the storage system. Each module can store 1.38 kWh. Thus, the system capacity is 689.7 kWh. We comment that  $\phi = 0$  overestimates the energy needs, while  $\phi = 1$  underestimates them. Actual values are in the range  $\phi = 0.1 \div 0.25$ . Fig. 5 shows the yearly evolution of the storage level with the daily peak net power flow  $P_{net}$ .

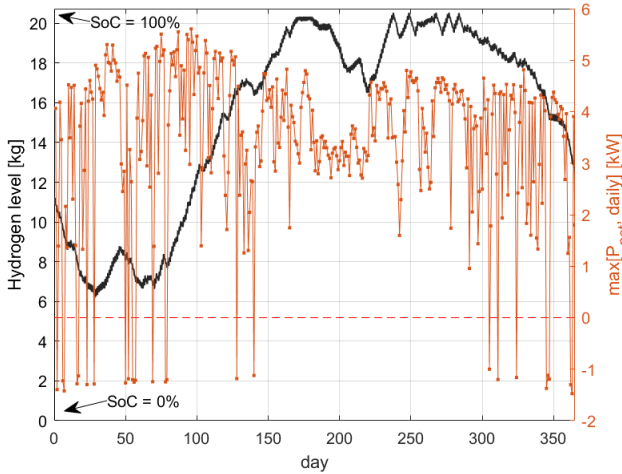


Fig. 5. Yearly evolution of the hydrogen level [kg] and the daily absolute peak of the net power flow [kW] for the baseline scenario.

The PV system has a peak power of 5.88 kW and occupies an area of 29.4 m<sup>2</sup>, while the yearly consumption (electricity, heating and cooling) is 4,305.9 kWh. Two electrolyzers are used in parallel, while one fuel cell is used. The SSR is equal to 99.98%, confirming total self-sufficiency throughout the year with only 0.83 kWh retrieved from the grid. 105.1 kg of hydrogen is produced in the year, while 103.6 kg are used. In fact, the final SoC is 60.2%, higher than the initial 50%. This is due to the conservative way of sizing the PV system, with  $\phi = 0$ .

The lower SoC is found on Jan. 28<sup>th</sup> at 29.8%, widely conservative as a lower margin. The higher SoC is found repeatedly between Aug. 25<sup>th</sup> and Oct. 10<sup>th</sup> at 1. This implies that 548.7 kWh of energy is sold to the grid. The compressor consumes only 67.5 kWh in the year, while the storage electric heater was never used in the year, i.e., the desorption was always fast enough.

The PBP is estimated at 41.9 years, with a total initial investment of 128.18 k€. The high PBP is due to the low savings and low consumptions, compared with a high

investment cost for the metal hydride. Fig. 6 shows the breakdown of the CAPEX costs. The MH dominates and accounts for 37.9% of the total initial investment, while the fuel cell module follows at 10.6%.

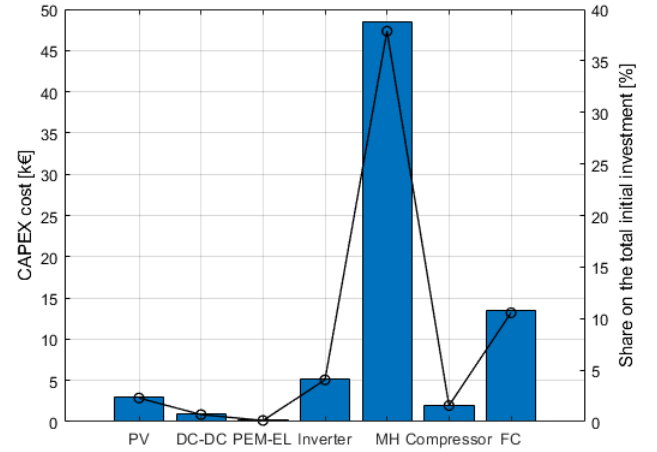


Fig. 6. Breakdown of CAPEX costs for the baseline scenario (Rome,  $n = 500$ , 1 apartment).

#### 3.2 Sensitivity analysis to climate zones

We analyze the same system (689.7 kWh storage capacity) in four other climate zones, namely cold, cooling base, moderate, and hot. Tab. 1 shows a comparative summary of the results.

Table 1: Yearly consumption, PV nominal power, total initial investment cost, payback period of the storage system and self-sufficiency ratio for five different climate zones.

zone	$E_{year}$ [kWh]	PV [kW]	$G_{tot}$ [k€]	PBP [year]	SSR [%]
Warsaw	4,664.9	8.84	136.05	34.6	79.90
Athens	4,823.1	6.24	128.43	37.3	97.16
Malaga	3,401.7	3.79	120.99	57.0	99.98
Rome	4,305.9	5.88	128.18	41.9	99.98
Larnaca	5,259.5	5.93	128.03	33.3	96.65

In the cold climate (Warsaw), the maximum SoC throughout the year spans the whole summer at around 84%. It doesn't reach 100% because of the high consumption load that increases the temperature and the equilibrium pressure, thus slowing down or hindering further absorption. Because of this, 3,120.7 kWh are sold to the grid in the year.

Storage systems located in Malaga and Larnaca yield the lowest PBP overall, at around 33.3 years, still very high. Furthermore, the moderate consumption values in Malaga only allow for a slightly lower investment cost, at around 120.99 k€. This is due to a smaller PV system.

A cold climate like in Warsaw yields a 17.42% lower PBP compared to the baseline scenario but also a 20.1%

lower SSR, in spite of a 50.3% bigger PV system. The lower PBP is due to the relatively high remunerations derived from energy sent to the grid, equal to 33.4% of the total yearly cash inflow. This also explains the lower SSR.

Yearly consumptions are relatively close for each climate zone, with the exception of Malaga and Larnaca which present a  $\pm 20.9\%$  deviation from the baseline case. This means that differences in PV peak power and systems costs are mainly due to the distribution of energy generation and consumption throughout the year and the day.

### 3.3 Sensitivity analysis to the number of apartments

The baseline case is set for one apartment. The system behavior is mainly linear, so that we can assume that all results collected can be scaled up with the number of apartments to be served in the community. For instance, a residential building in Rome would require a PV system of 5.88 kW/apt. while in Malaga it would be 3.79 kW/apt. The main source of non-linearity is represented by the evolution of PEM-EL and FC efficiencies as a function of the net input power flow. For the purpose of this paper, we can disregard this effect.

### 3.4 Sensitivity analysis to the storage capacity

Fig. 7 shows the yearly evolution of hydrogen level and daily peaks of net power flows when  $n = 250$  and the storage capacity is 344.9 kWh.

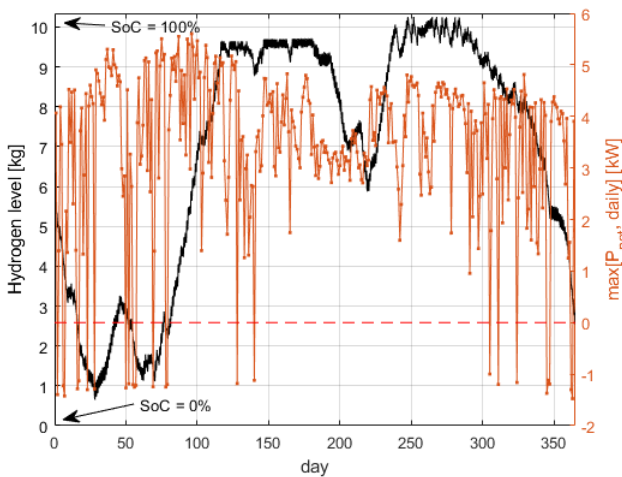


Fig. 7. Yearly evolution of the hydrogen level [kg] and the daily absolute peak of the net power flow [kW] when  $n=250$  in Rome.

SSR does not change sensibly (99.95) but the PBP decreases to 22.5 years, thus suggesting that a number of modules  $n$  equal to 250 is more efficient in terms of system volume, weight and economy-wise. We comment that the SoC at the end of the year is 24.7%, lower than

the initial value of 50%. This means that, in order for this system to be self-sufficient through the years, we have to integrate with  $(0.5 - 0.247)MH_C/\overline{\eta_{EL}} = 143.7$  kWh, where  $MH_C$  is the storage capacity and  $\overline{\eta_{EL}}$  is the average electrolyzer efficiency. This can be done at a moderate price of  $\sim 35.9$  € at a price of 25 c€/kWh. By doing so, the SSR would negligibly decrease to 96.6%, still confirming the substantial self-sufficiency of the residential building. The optimization of the initial and final SoC through the years requires an iterative solution of the algebraic problem, since the efficiency of PEM-EL and FC are in turn a function of the absorption and desorption kinetics.

Fig. 8 shows the yearly evolution of hydrogen level and maximum daily net power flows when  $n = 125$  and the storage capacity is 172.4 kWh.

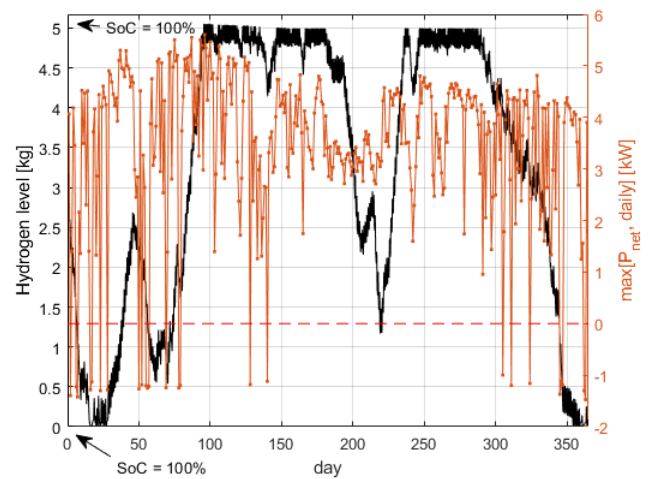


Fig. 8. Yearly evolution of the hydrogen level [kg] and the daily absolute peak of the net power flow [kW] when  $n=125$  in Rome.

SSR is still very high (98.1%) but the PBP decreases to 11.2 years. Furthermore, we comment that the SoC drops to 0% at day 355. This means that this storage system cannot sustain the energy consumptions of the building and is thus too small.

## 4. CONCLUSIONS

The work presents a techno-economic analysis of a low-emission residential building with local energy storage. Energy is produced in a local PV system while excess energy is stored in a metal hydride hydrogen storage system. An electrolyzer module, a fuel cell module and a reciprocating compressor ensures energy flow between the PV and the building. A sensitivity analysis is conducted on the system location, according to five different climate zones, the storage capacity, and the yearly consumption (i.e., the number of apartments to be served).

Results show that a 5.88 kWp PV system coupled with a 345 kWh storage system is fully capable of ensuring a zero-emission operation for each apartment in one year in Rome, or any city in a heating-based climate zone. The system thus needs a storage system with a capacity of 22 kg of hydrogen. A hot climate (e.g., Larnaca) increases the needed storage capacity to around 689.7 kWh, while a cold climate (e.g., Warsaw) only reaches a 79.9% self-sufficiency ratio at that storage capacity.

While costs remain relatively high when compared to compressed gas systems, the work demonstrates great advantages to battery energy storage systems, since these cannot reach storage characteristic periods larger than hours or a few days conveniently.

#### 4.1 Practical Implementation and Real-World Applications

The results of this study highlight the potential of MH – PCM hydrogen storage systems for enabling high self-sufficiency in residential buildings across diverse climates. While the current costs are a major barrier, the findings suggest several real-world application pathways: **(i)** Pilot residential and community-scale project, since the system is especially suited for demonstration in off-grid or near-zero-energy buildings; **(ii)** integration with district energy and community microgrids, where scaling from single apartments to multi-apartment complexes or neighborhoods would improve economies of scale and better amortize high upfront investments; **(iii)** alignment with policy and incentive schemes, since deployment can be accelerated in regions where subsidies for hydrogen technologies, carbon taxes, or resilience requirements make long-duration storage economically competitive. Finally, beyond residential buildings, MH–PCM hydrogen storage can be implemented in commercial facilities with high heating/cooling demand.

#### ACKNOWLEDGEMENT

- ECS0000024RomeTechnopole, UPB83C22002820006, National Recovery and Resilience Plan (NRRP) Mission 4 Component 2 Investment 1.5, funded by the European Union-NextGenerationEU.
- PRIN P20223JMB3-Modeling and optimization of sustainable hydrogen refueling infrastructures (HyREFI).

#### REFERENCE

- [1] Solar Power Europe, *The Rise of Solar PV in the EU - key facts*, url: [Total EU-27 Solar PV capacity: a growth story - SolarPower Europe](#). Last visited, 03/09/2025.
- [2] Goebel C., Cheng V., Jacobsen H.-A., *Profitability of Residential Battery Energy Storage Combined with Solar Photovoltaics*, *Energies* 10 (7) (2017), 957.
- [3] Rosati A., Facci A. L., Ubertini S., *Techno-economic analysis of battery electricity storage towards self-sufficient buildings*, *Energy Conversion and Management* 256 (2022), 115313.
- [4] Linggang Jin, Mosè Rossi, Andrea Monforti Ferrario, Francesca Mennilli, Gabriele Comodi, *Designing hybrid energy storage systems for steady green hydrogen production in residential areas: A GIS-based framework*, *Applied Energy*, Volume 389, 2025, 125765.
- [5] E. H. Observatory. *Levelized cost of hydrogen calculator*, 2024. <https://observatory.clean-hydrogen.europa.eu/tools-reports/levelised-cost-hydrogen-calculator>.
- [6] *Performance Analysis of a Zero-Energy Building Using Photovoltaics and Hydrogen Storage*, Evangelos Bellos, Panagiotis Lykas, Christos Tzivanidis, *Appl. Syst. Innov.* **2023**, 6(2), 43
- [7] L. Abdolmaleki, A. Jahanbin, U. Berardi, *Towards standalone commercial buildings in the Mediterranean climate using a hybrid metal hydride and battery energy storage system*, *Journal of Building Engineering*, Volume 96, 2024, 110567. <https://doi.org/10.1016/j.jobee.2024.110567>.
- [8] IEA (2008), *Energy Efficiency Requirements in Building Codes: Policies for New Buildings*, IEA, Paris <https://www.iea.org/reports/energy-efficiency-requirements-in-building-codes-policies-for-new-buildings>
- [9] GFE Titanium, Energy supply with Hydralloy® C, [https://www.gfe.com/02\\_produkte\\_loesungen/01\\_legierungen/PDB/HYDRALLOY-C\\_2019-929\\_-2005-169\\_2004-732-\\_V8.pdf](https://www.gfe.com/02_produkte_loesungen/01_legierungen/PDB/HYDRALLOY-C_2019-929_-2005-169_2004-732-_V8.pdf)
- [10] M. Maggini, G. Falcucci, A. Rosati, S. Ubertini, A. L. Facci, *Non-dimensional numerical analysis of coupled Metal Hydride-Phase Change Material hydrogen storage system*, *Journal of Energy Storage*, Volume 93, 2024.
- [11] M. Maggini, A. L. Facci, G. Falcucci, S. Ubertini, *Numerical Modeling of Metal Hydride-Phase Change Material Hydrogen Storage Systems with Increased Heat Exchange surface area*, *Applied Energy*, Volume 378, Part A, 2025, 124725, ISSN 0306-2619
- [12] M. Maggini, G. Falcucci, A. L. Facci, S. Ubertini, *Enhancing Metal Hydride – Phase Change Material*

*Hydrogen Storage Systems Efficiency with Expanded Graphite*, Energy Proceedings, Vol. 49 2024

[13] M. Maggini, A. L. Facci, G. Falcucci, S. Ubertini, *Simulation-Driven Optimization of Metal Hydride-Packed Hydrogen Storage Systems for Enhanced Performance*, Energy Proceedings, Vo. 39 2024

[14] B. Talagañis, G. Meyer, P. Aguirre, *Modeling and simulation of absorption desorption cyclic processes for hydrogen storage-compression using metal hydrides*, Int. J. Hydrog. Energy 36 (2011).

[15] L. Tribioli, R. Cozzolino, M. Barbieri, *Optimal control of a re powered vehicle: Plug-in fuel cell against plug-in hybrid electric powertrain*, in: *Proceedings of the International Conference on Numerical Analysis and Applied Mathematics 2014*, 2015, p. 570014.

[16] Eurostat, Electricity price statistics (2024), [https://ec.europa.eu/eurostat/statistics-explained/index.php?title=Electricity\\_price\\_statistics](https://ec.europa.eu/eurostat/statistics-explained/index.php?title=Electricity_price_statistics)

[17] Y. Zhang, A. Lundblad, P. E. Campana, J. Yan, *Comparative Study of Battery Storage and Hydrogen Storage to Increase Photovoltaic Self-sufficiency in a Residential Building of Sweden*, in *Applied Energy Symposium and Forum, REM2016*, Energy Procedia 103 (2016)